

The 8th International Conference on MPGDs

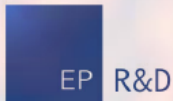
Robust photocathodes and spatial resolution studies of resistive PICOSEC Micromegas precise-timing detectors

Djunes Janssens and Marta Lisowska

On behalf of the PICOSEC Micromegas Collaboration

djunes.janssens@cern.ch

October 15th, 2024

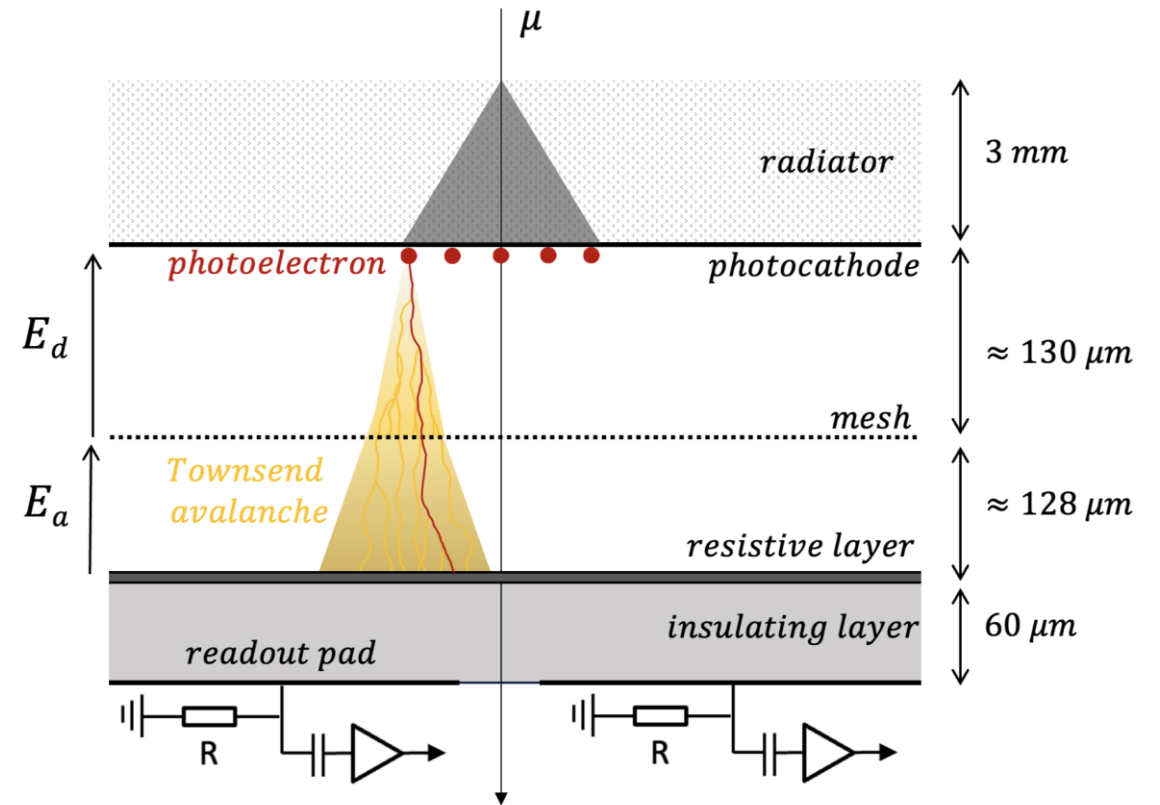


Introduction

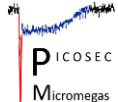
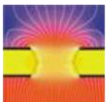
To enable the sub-25 ps PICOSEC Micromegas precise-timing detector to perform effectively under the demanding conditions of physics experiments, we are adapting its design to improve robustness.

Outline:

- Resistive Plane PICOSEC Micromegas
 - Single-Channel Prototype
 - Increased Readout Granularity for Spatial Resolution
 - Multi-Pad Prototype with Vertical Charge Evacuation
- Robust Photocathodes
 - DLC
 - B4C
 - Graphene
- Towards an Applicable Detector
- Conclusion



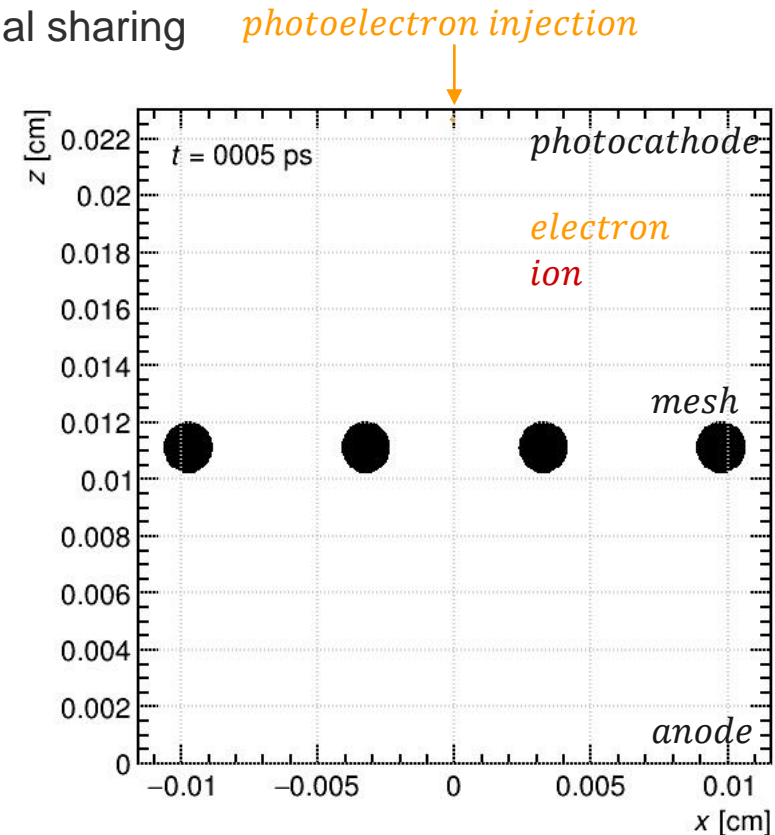
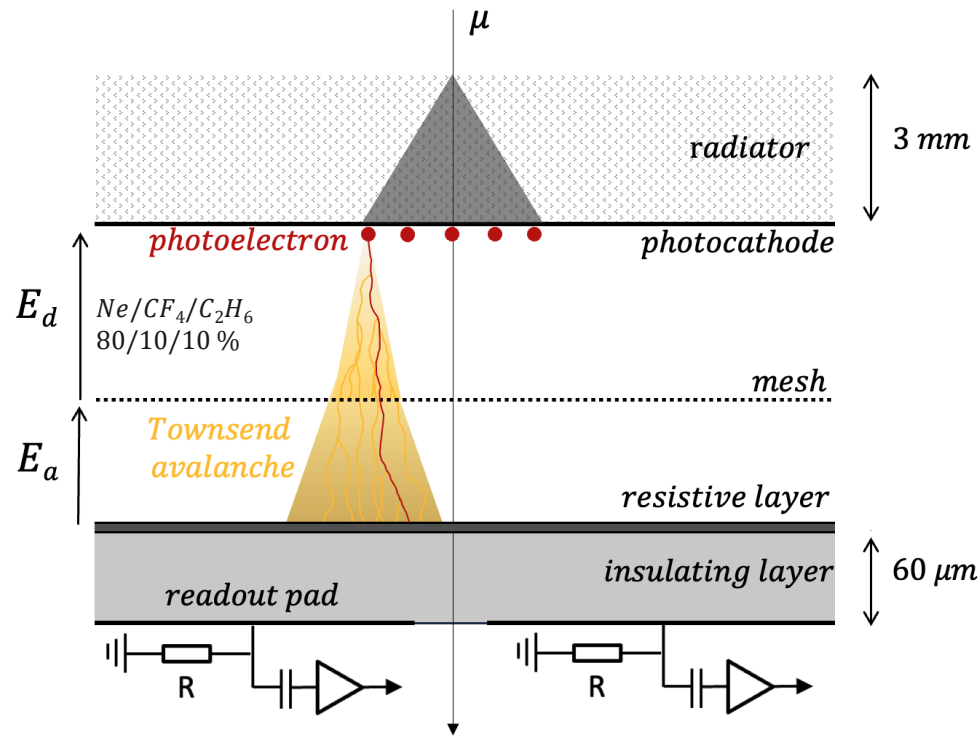
Resistive plane PICOSEC Micromegas



Resistive PICOSEC Micromegas

A resistive layer is introduced in both single- and 100-channel readout structures to enhance the detector's robustness while maintaining a timing resolution of under 25 ps. These slightly conductive materials offer:

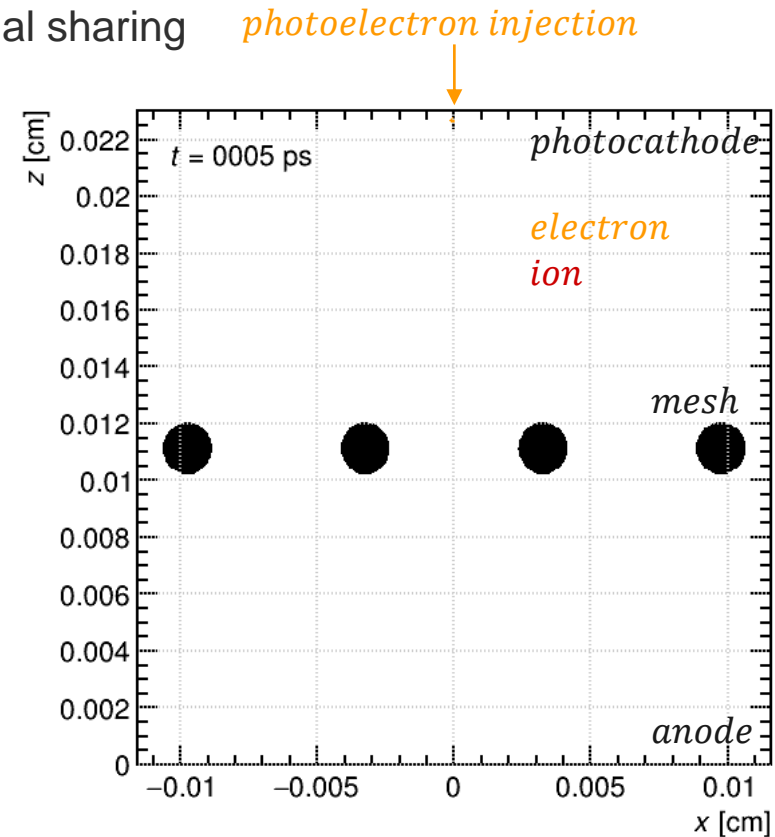
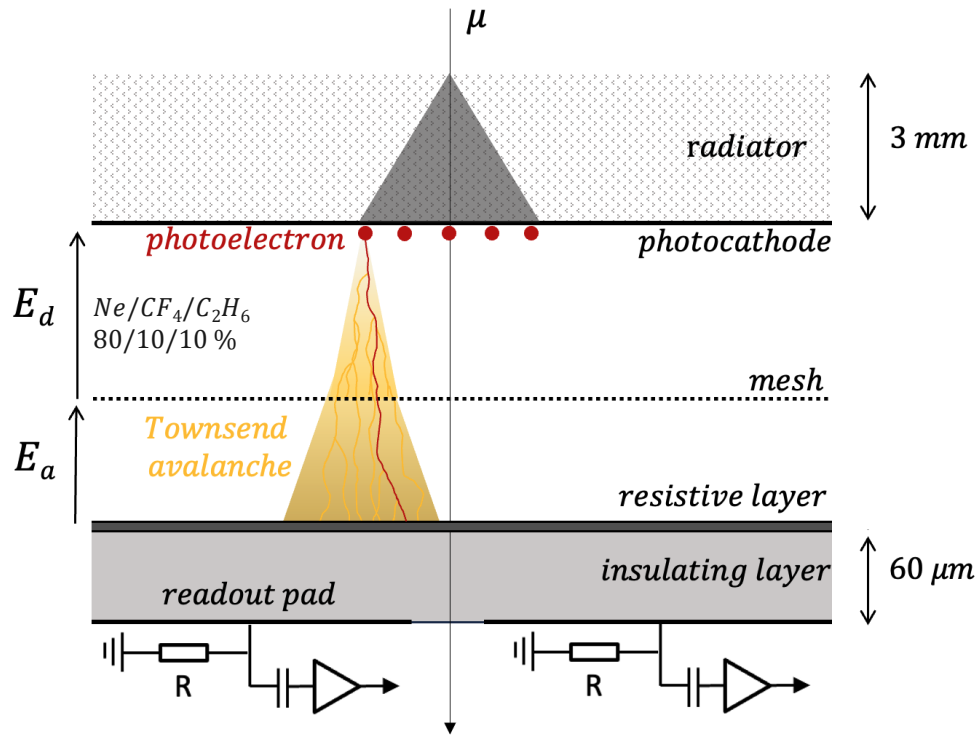
- More stable operation by quenching discharges
- Potentially improved position reconstruction through increased signal sharing



Resistive PICOSEC Micromegas

A resistive layer is introduced in both single- and 100-channel readout structures to enhance the detector's robustness while maintaining a timing resolution of under 25 ps. These slightly conductive materials offer:

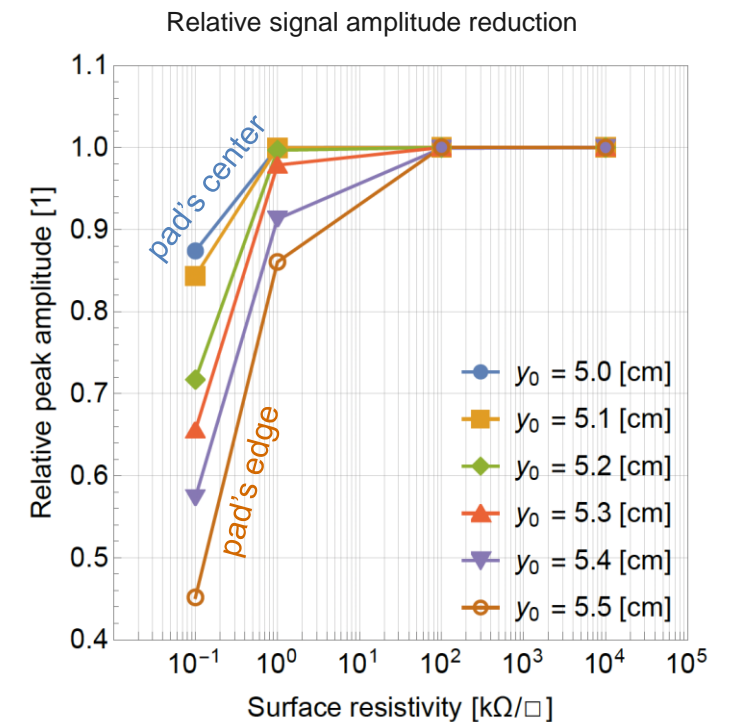
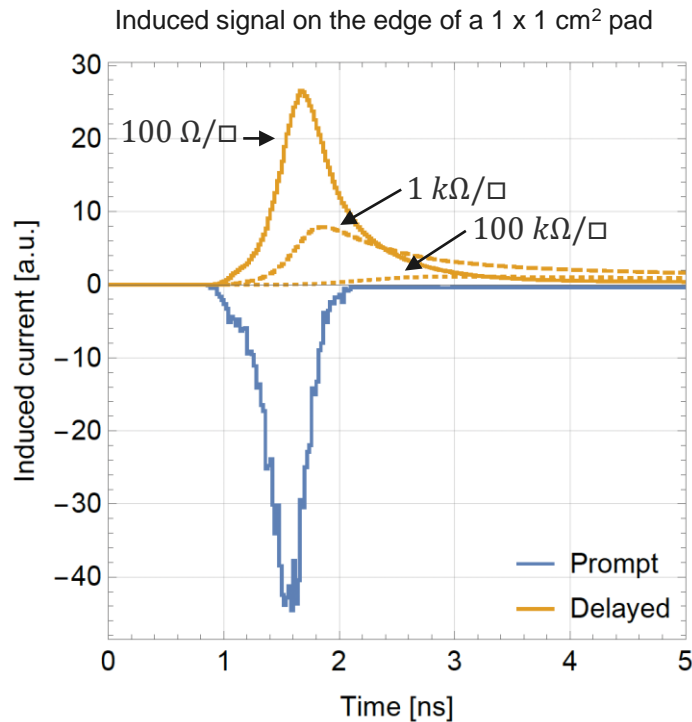
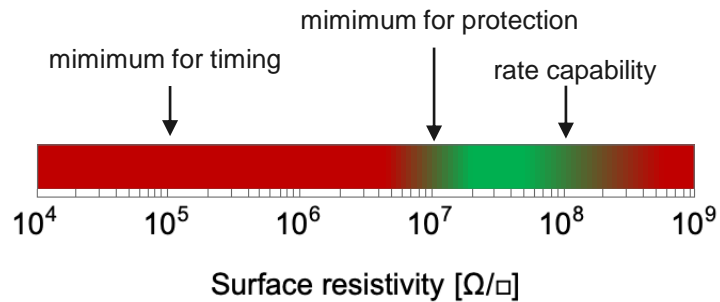
- More stable operation by quenching discharges
- Potentially improved position reconstruction through increased signal sharing



Resistive PICOSEC Micromegas

A surface resistivity of $20 \text{ M}\Omega/\square$ was chosen to ensure that:

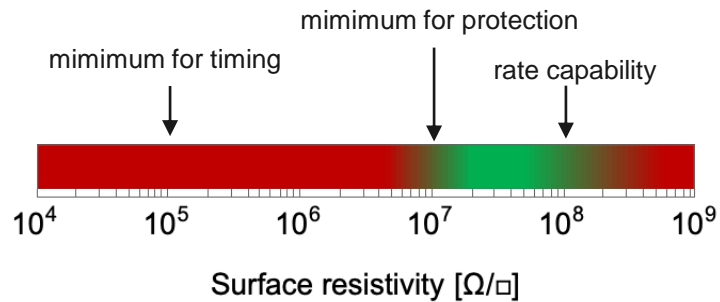
- the leading edge of the signal is minimally affected by the delayed component,
- the rate capability estimation,
- the protection against discharges.



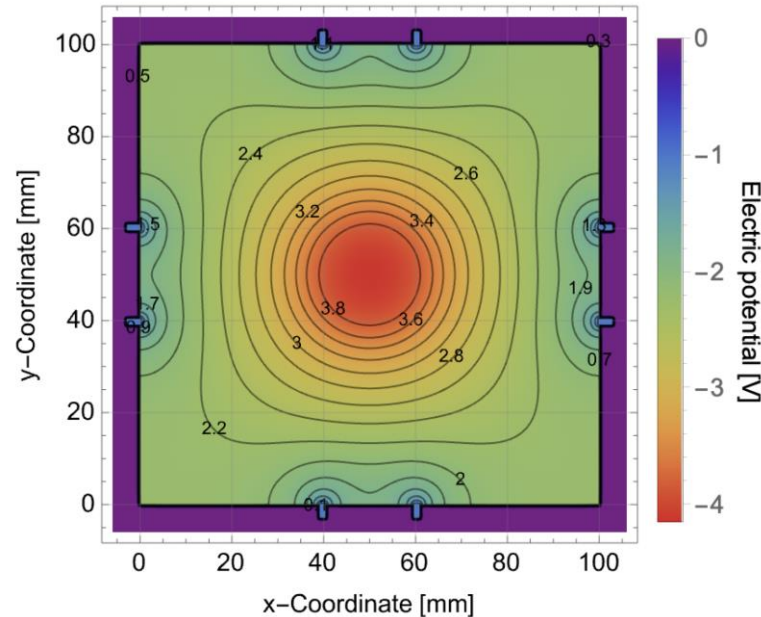
Resistive PICOSEC Micromegas

A surface resistivity of $20 \text{ M}\Omega/\square$ was chosen to ensure that:

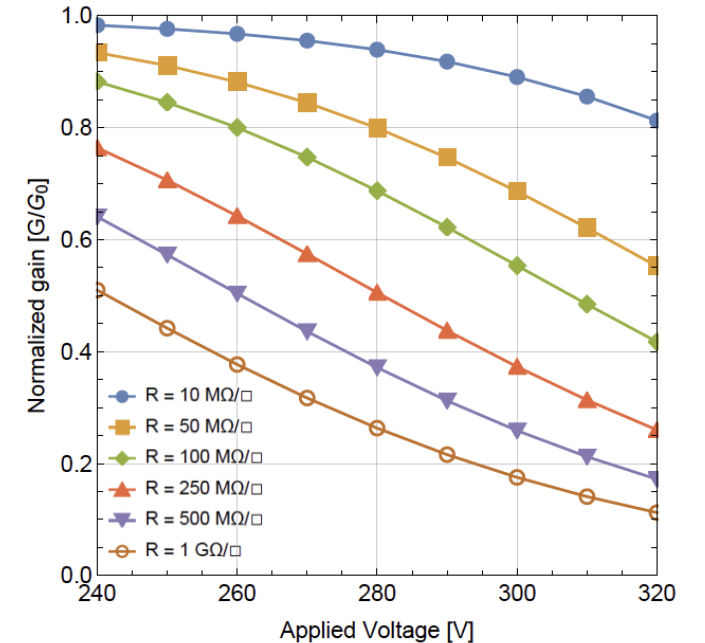
- the leading edge of the signal is minimally affected by the delayed component,
- **the rate capability estimation,**
- the protection against discharges.



Simulated voltage drop for $\Phi = 6 \cdot 10^5 \text{ cm}^{-2}\text{s}^{-1}$ pion beam



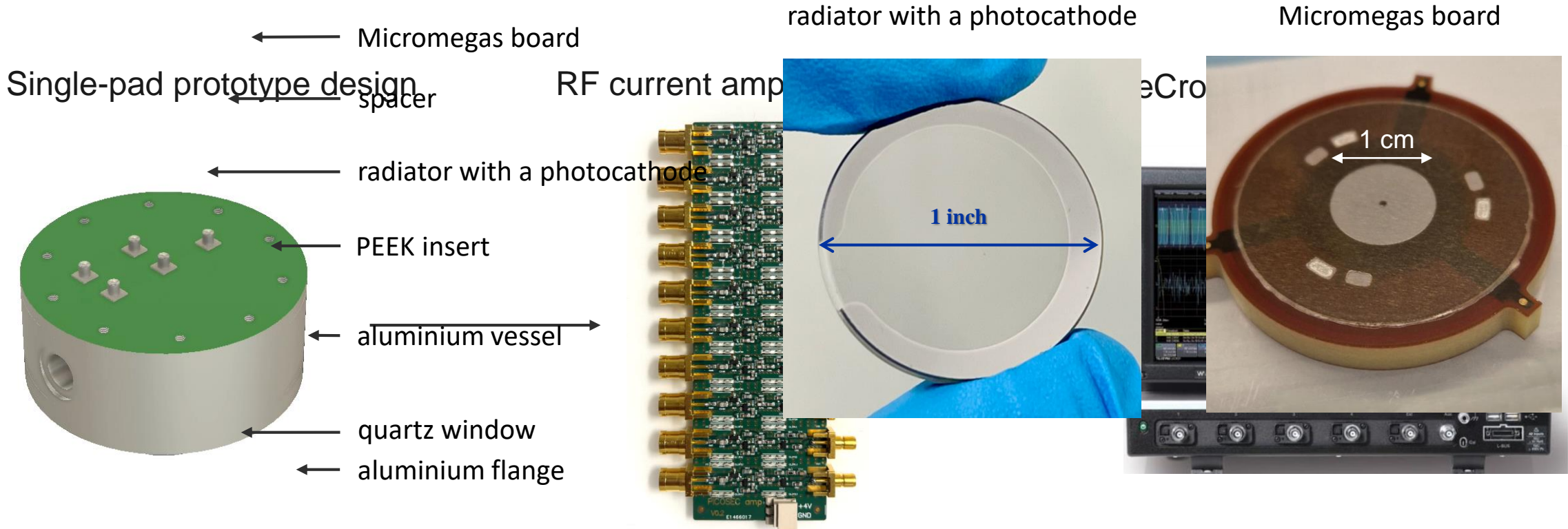
Simulated amplification drop from $\Phi = 6 \cdot 10^5 \text{ cm}^{-2}\text{s}^{-1}$ pion beam



Single channel resistive PICOSEC Micromegas

After production, the timing performance of the resistive single-pad detector for fully contained events was measured using custom-built current amplifiers and a 10 GS/s sampling oscilloscope.

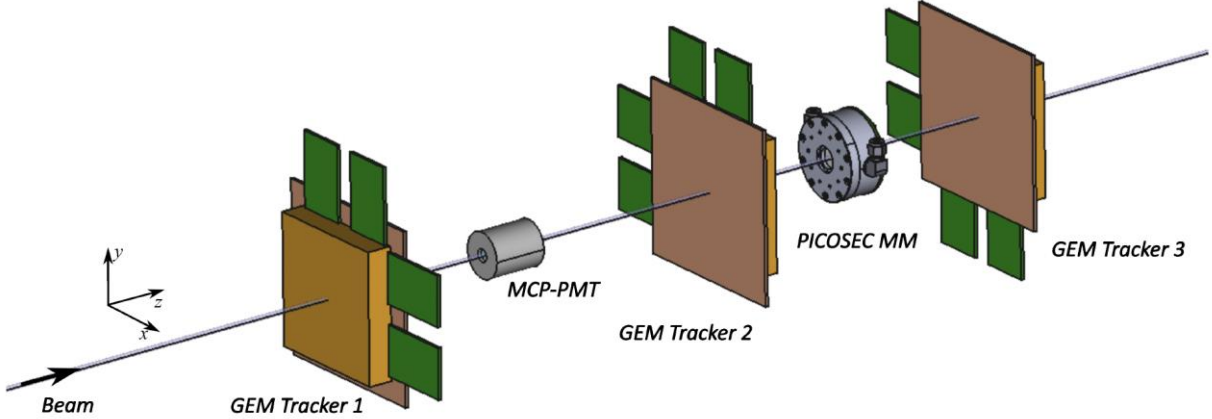
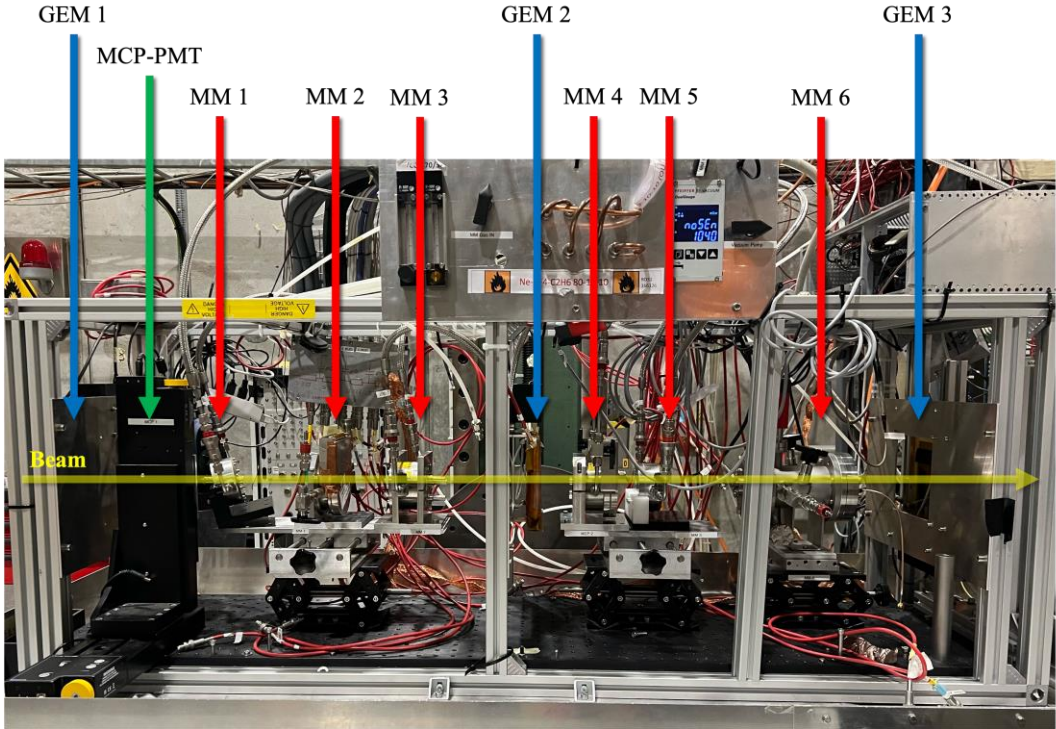
outer board with
spring loaded pins



Single channel resistive PICOSEC Micromegas

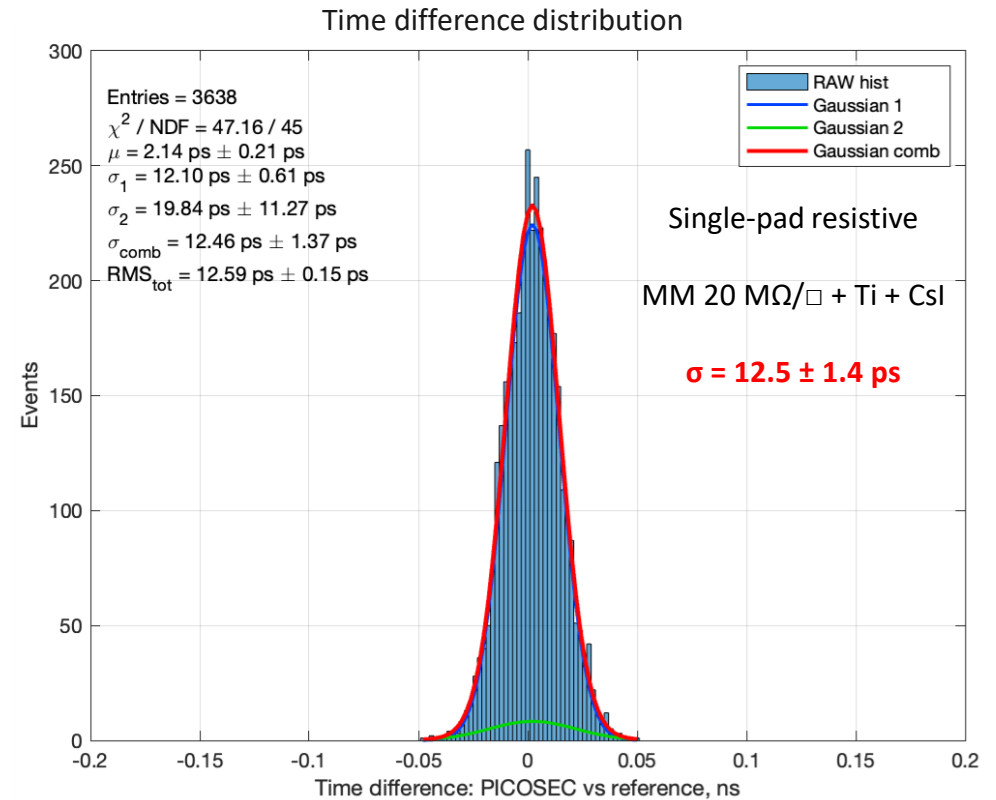
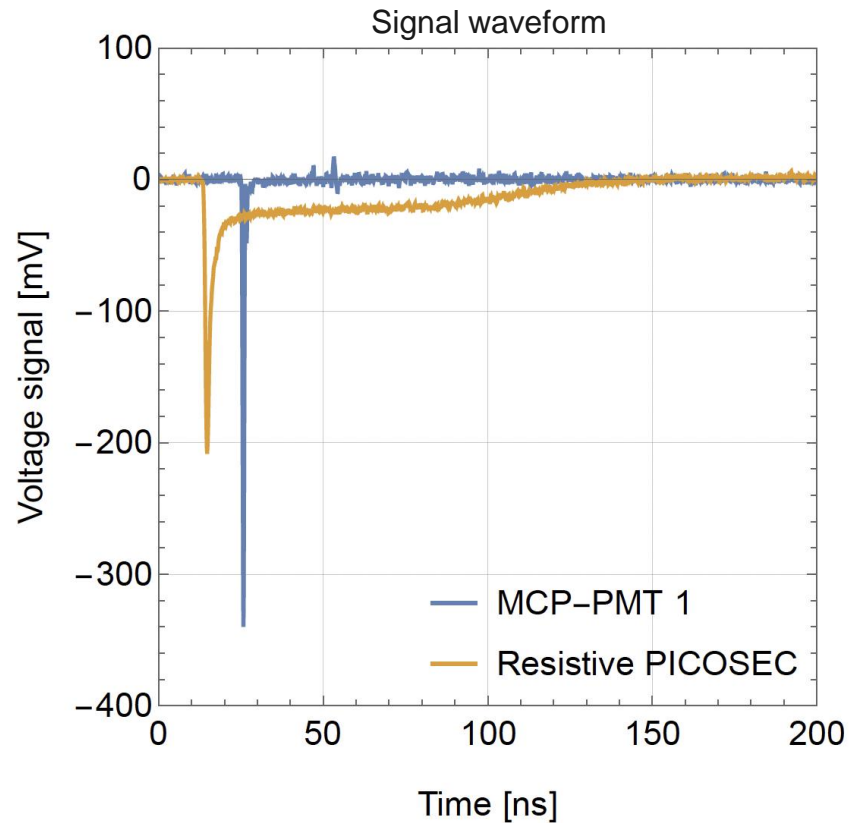
This prototype, along with several others, was tested in both the lab and the CERN SPS H4 beamline using 150 GeV/c muons.

By utilizing tracking information from GEMs and timing information from MCP-PMTs, the timing performance could be measured.



Single channel resistive PICOSEC Micromegas

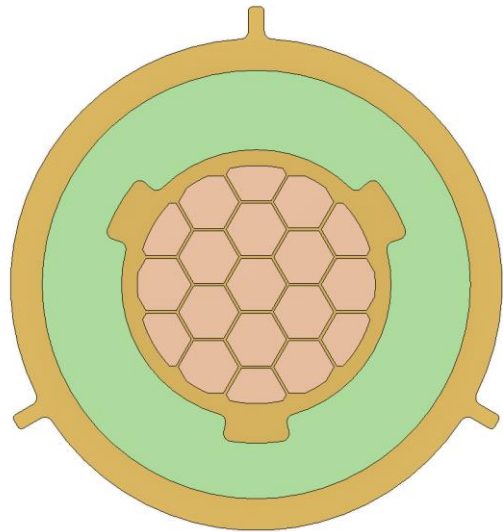
The detector with 10 mm ϕ active area demonstrated equivalent performance compared to a non-resistive prototype, achieving a time resolution of $\sigma = 12.5 \pm 1.4$ ps.



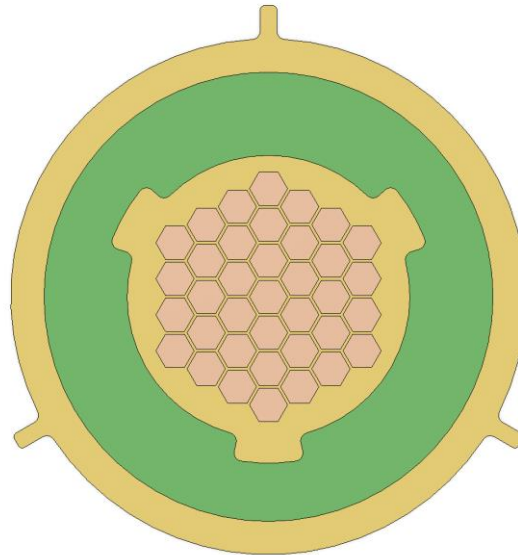
Increase readout granularity for spatial resolution

To investigate potential improvements in spatial resolution, two sets of resistive PICOSEC Micromegas prototypes with increased granularity and a 15 mm active area were produced and tested.

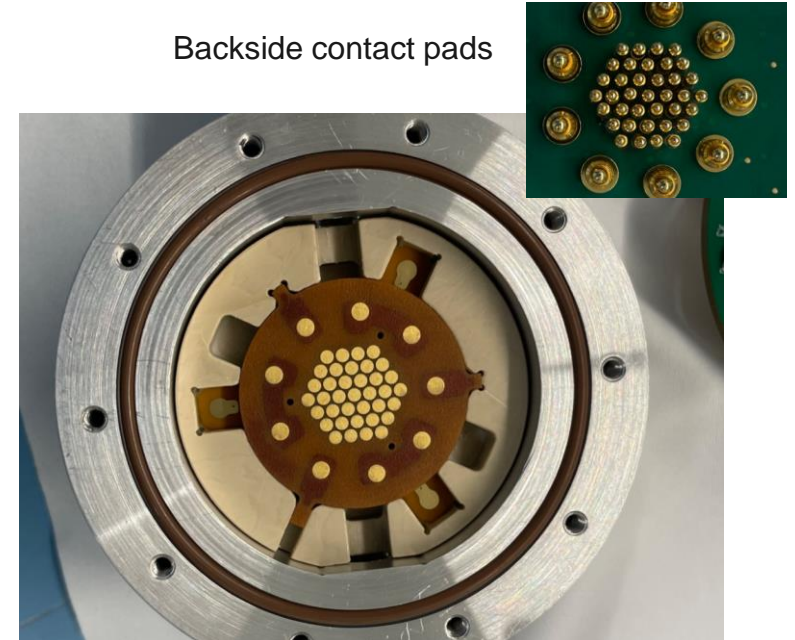
19 pads with 3.5 mm pitch



37 pads with 2.2 mm pitch



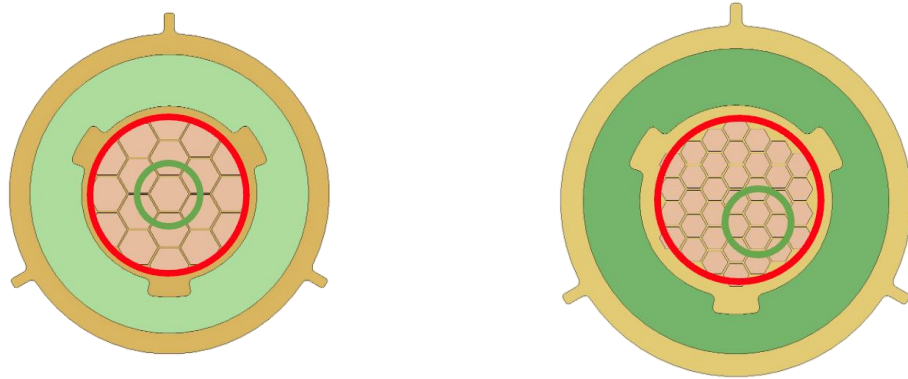
Backside contact pads



The pads were read out using a SAMPIC waveform TDC, while an MCP-PMT (timing reference) scanned across the active area (self-triggered in coincidence with the reference).

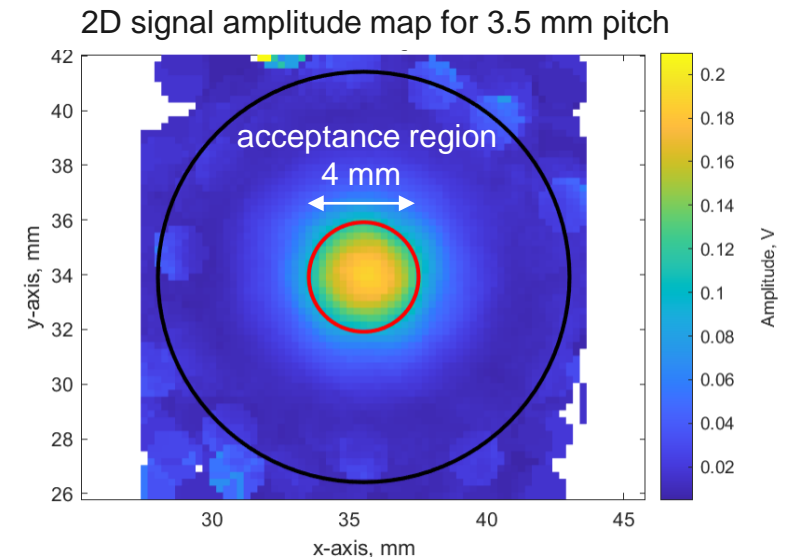
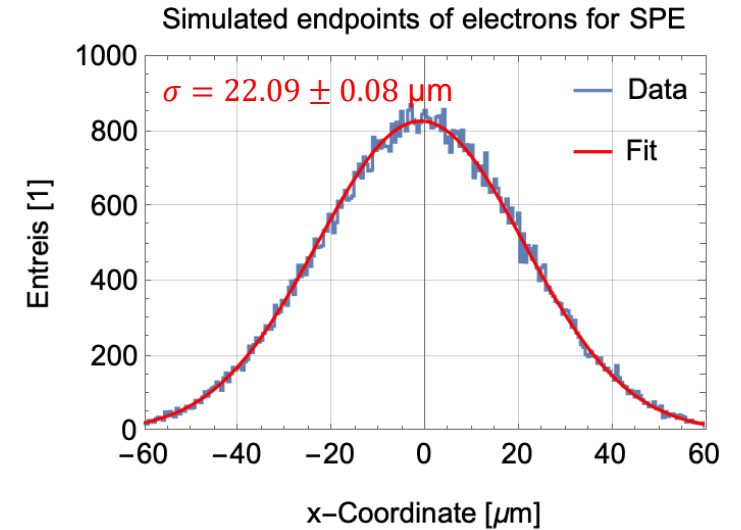
Increase readout granularity for spatial resolution

For the 3.5 mm readout pad pitch, comparable timing performance was observed on the central pad, despite only having partially contained events, with most charge centered around the particle trajectory.



	single pad	medium granularity	high granularity
pad pitch [mm]	15.0	3.5	2.2
mean signal ampl. [mV]	193	157.8	62.3
central pad σ_t [ps]	13.9	16.9 ± 0.15	28.3 ± 0.3
cluster size	1	4.0	3.6
x-residuals (full active area) [mm]	/	1.04	1.03
x-residuals (inner 6mm circle) [mm]	/	0.5	0.65

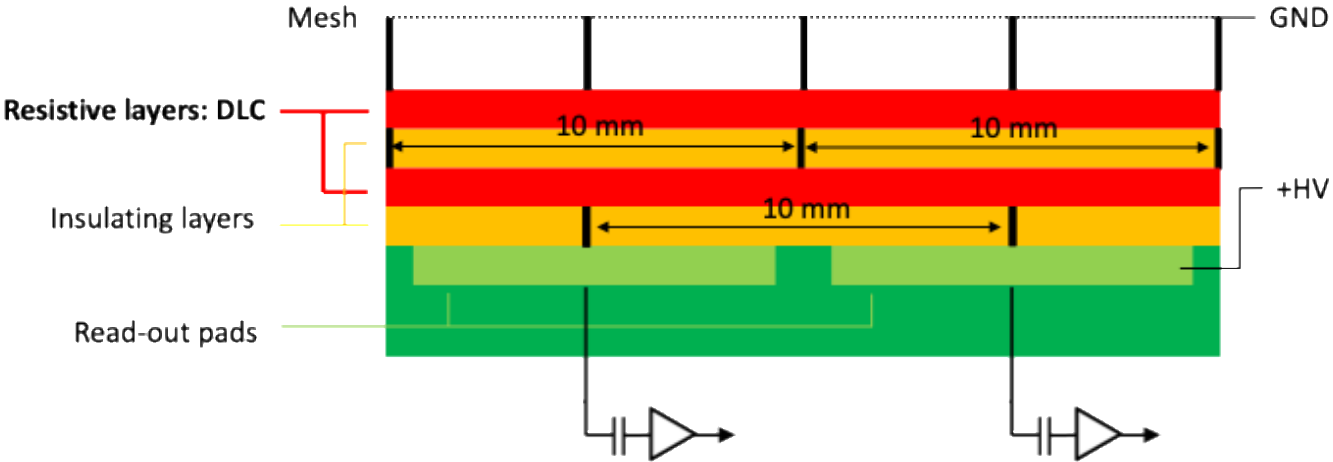
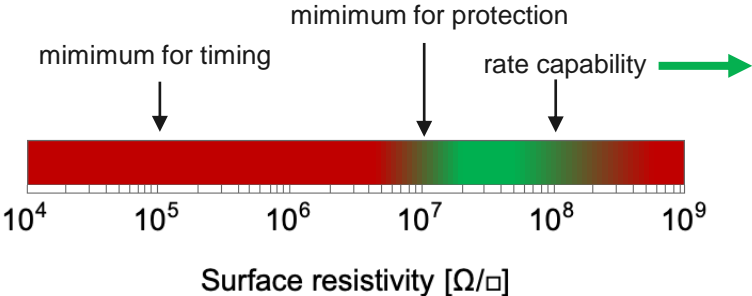
Both timing and spatial resolution are worse for the high granularity readout, most likely due to the smaller signal amplitudes.



Multi-pad prototype with vertical charge evacuation

The rate capability of resistive MPGDs is highly dependent on the charge evacuation scheme used. Various promising 'fast evacuation' configurations can be found within our community.

To enhance the rate capability of the 10 x 10 cm² resistive multi-pad design, a vertical charge evacuation configuration was developed, in contrast to the previous single DLC layer with horizontal evacuation.



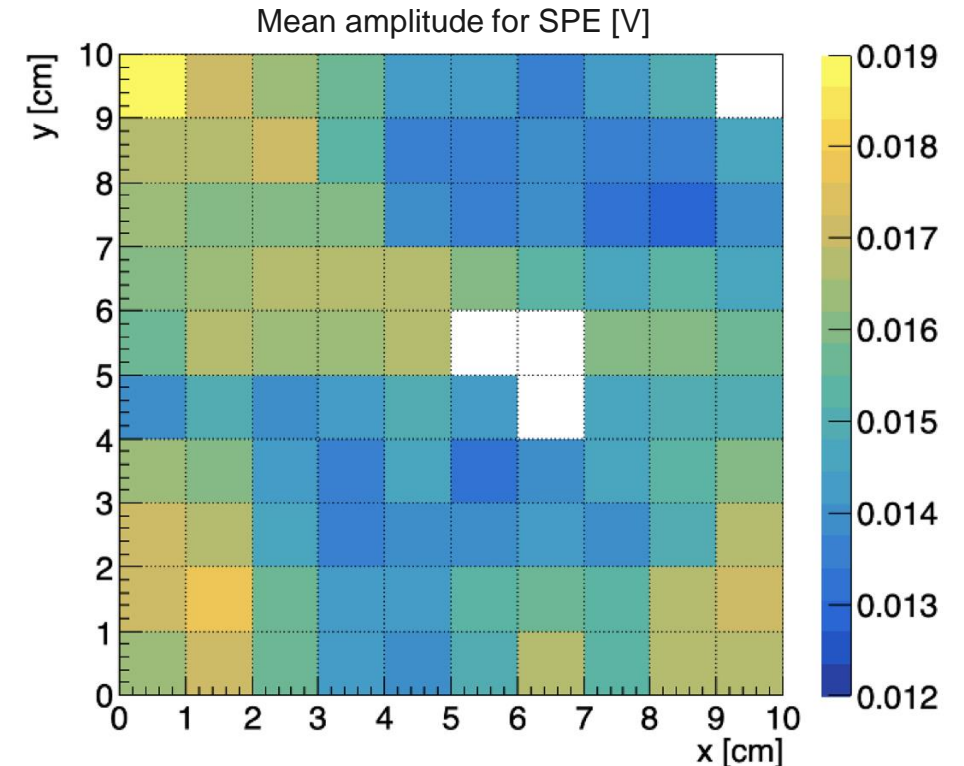
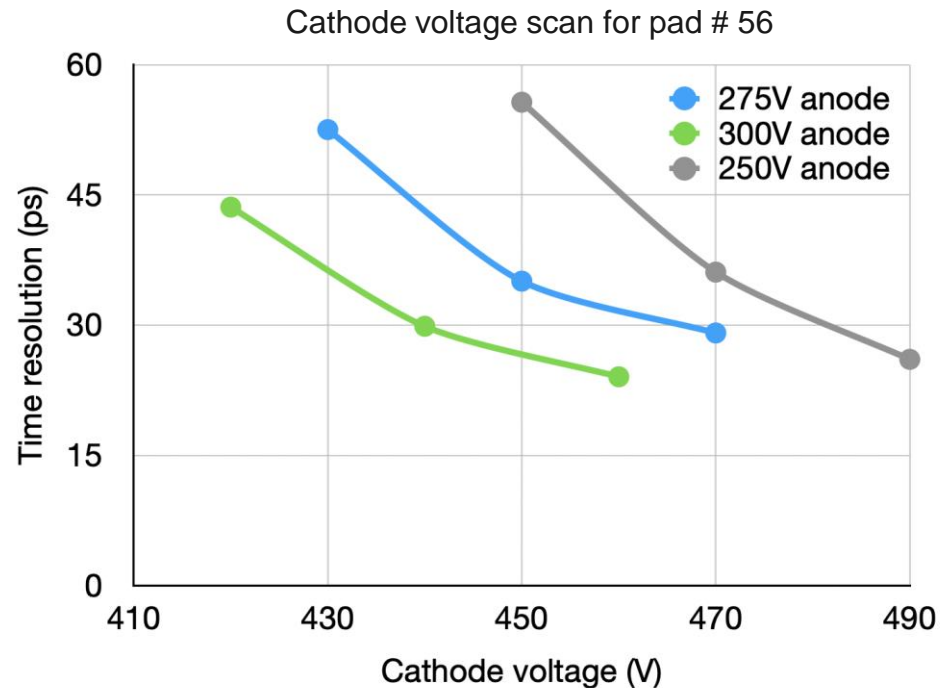
Multi-pad prototype with vertical charge evacuation

While the observed planarity of the MM board was $\sim 15 \mu\text{m}$ after bulking, this does not fully explain the magnitude of the non-uniform response observed across the active area.

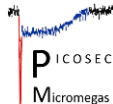
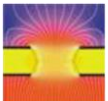
→ Possibly exacerbated by photocathode degradation!

Measured quantities for 150 GeV/c muons

<p><u>pad 19:</u> $\langle V \rangle = 91.8 \text{ mV}$ $\sigma_t = 22.1 \text{ ps}$</p>	<p><u>pad 56:</u> $\langle V \rangle = 50.6 \text{ mV}$ $\sigma_t = 29.1 \text{ ps}$</p>	<p><u>pad 12:</u> $\langle V \rangle = 97.2 \text{ mV}$ $\sigma_t = 21.5 \text{ ps}$</p>
<p><u>pad 89:</u> $\langle V \rangle = 99.3 \text{ mV}$ $\sigma_t = 19.1 \text{ ps}$</p>		<p><u>pad 82:</u> $\langle V \rangle = 104.2 \text{ mV}$ $\sigma_t = 19.1 \text{ ps}$</p>



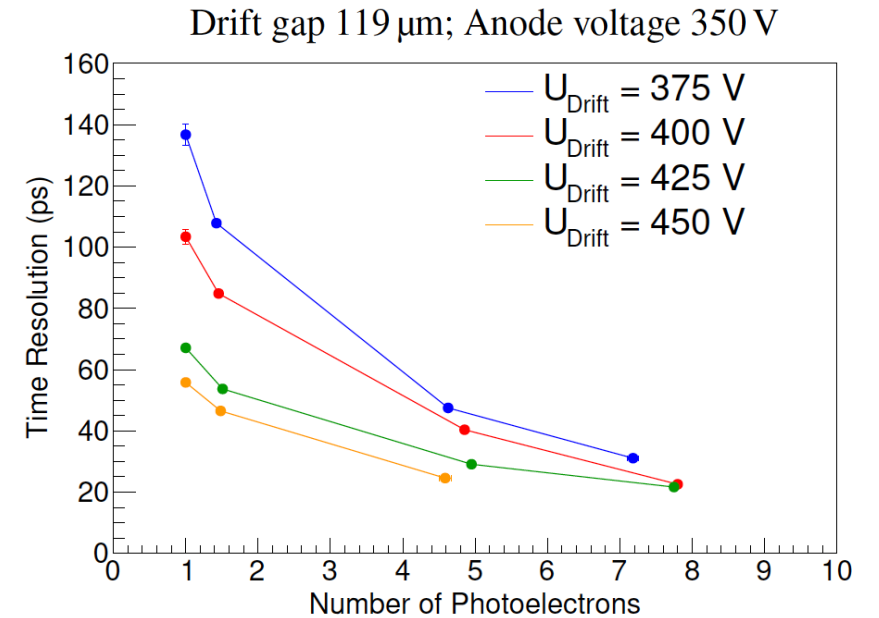
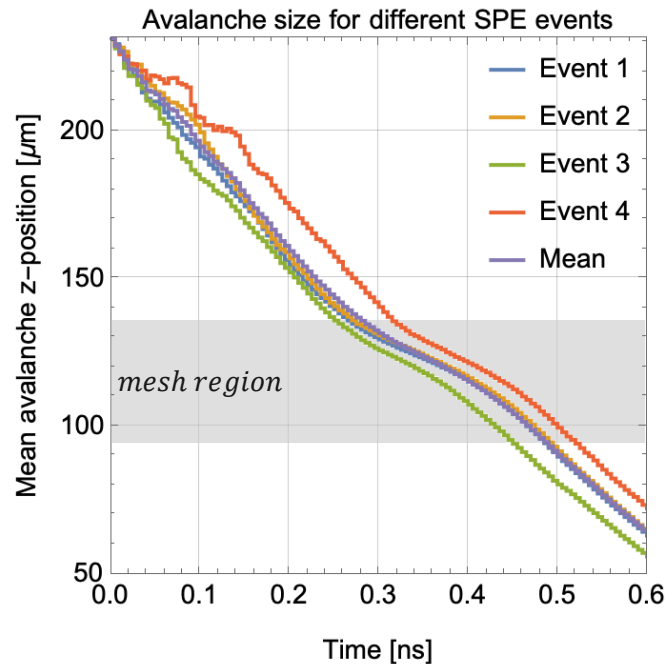
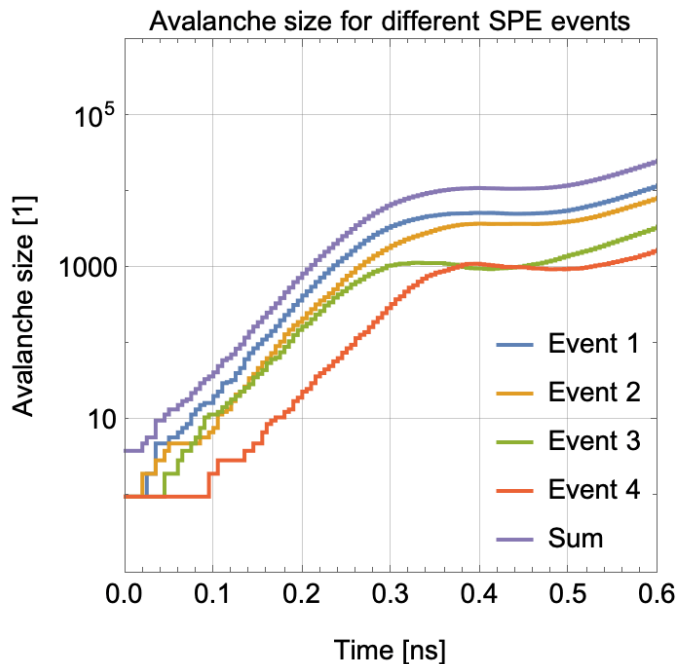
Robust photocathodes



Number of photoelectrons

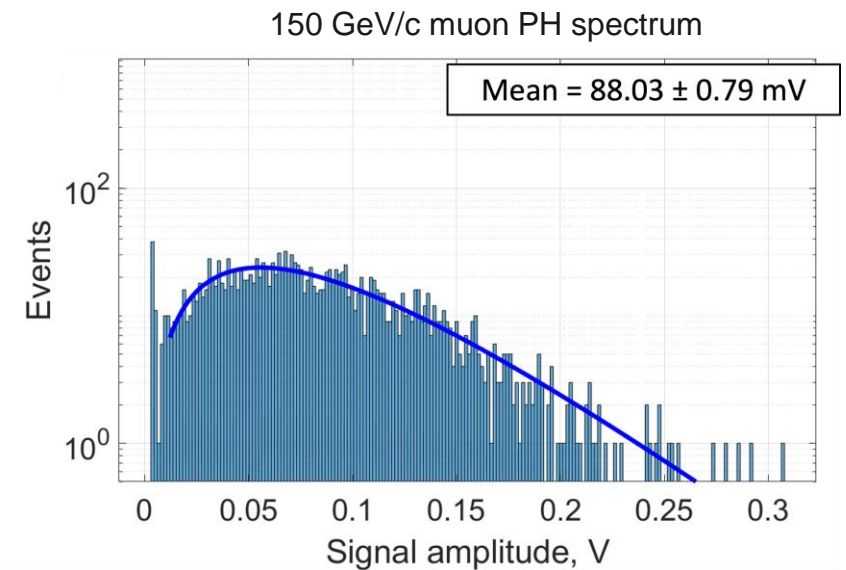
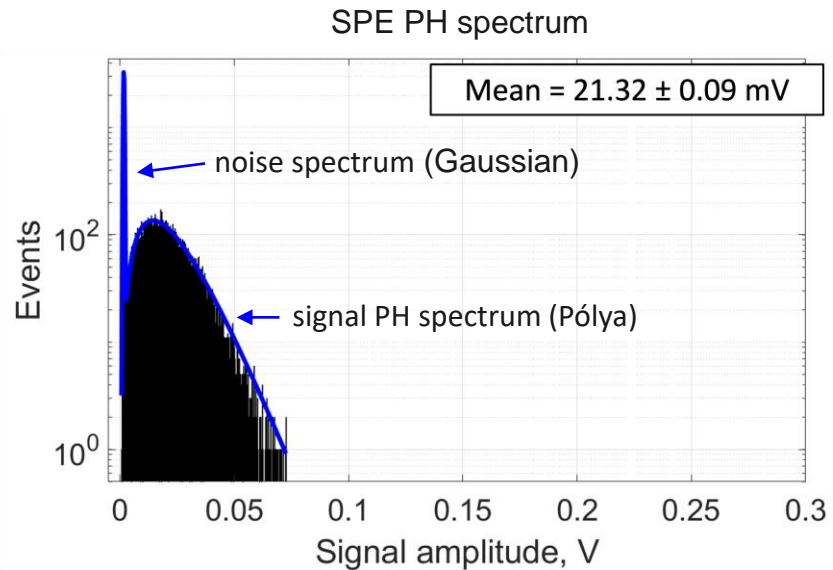
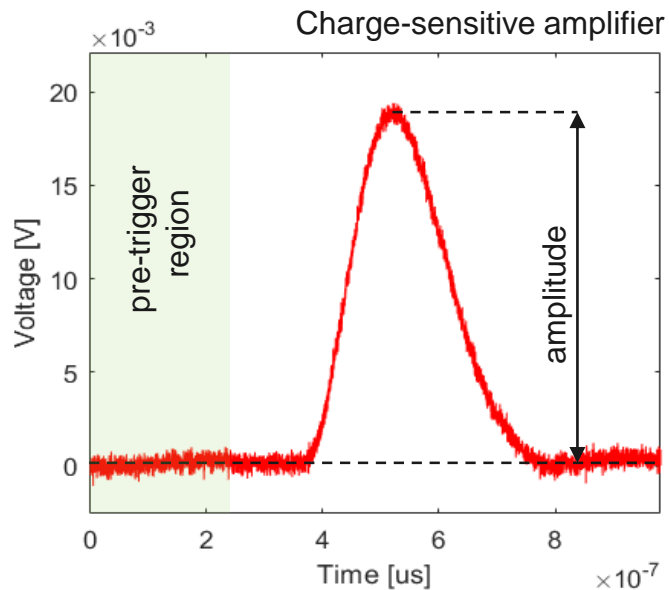
Given a particle crossing the radiator, the choice of photocathode affects the number of photoelectrons (PEs) produced, which is determined by its quantum efficiency. This, in turn, influences the time resolution, which depends on:

$$\text{timing resolution} \longrightarrow \sigma \propto \frac{\sigma_{SPE}}{\sqrt{N_{PE}}} \longleftarrow \begin{array}{l} \text{timing resolution for single PE} \\ \text{number of PEs} \end{array}$$



Number of photoelectrons

The average number of photoelectrons (NPE) is obtained by comparing the pulse heights of single photoelectron (SPE) events, measured with a UV LED, to those from multiple photoelectron measurements using a muon beam.



→ A photocathode with 3 nm Cr and 18 nm CsI produces over 12 photoelectrons per muon when combined with a 3 mm MgF₂ crystal.

Alternative Photocathodes to CsI

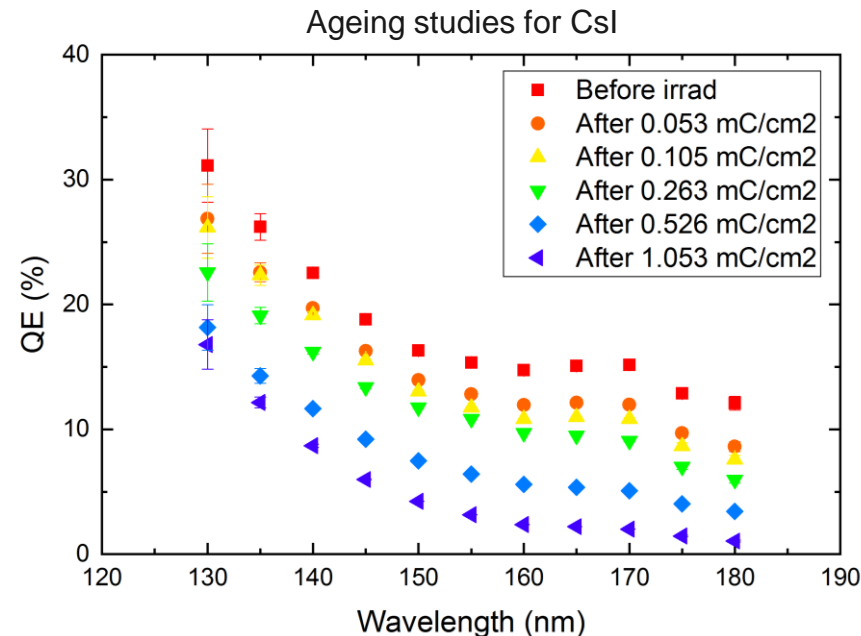
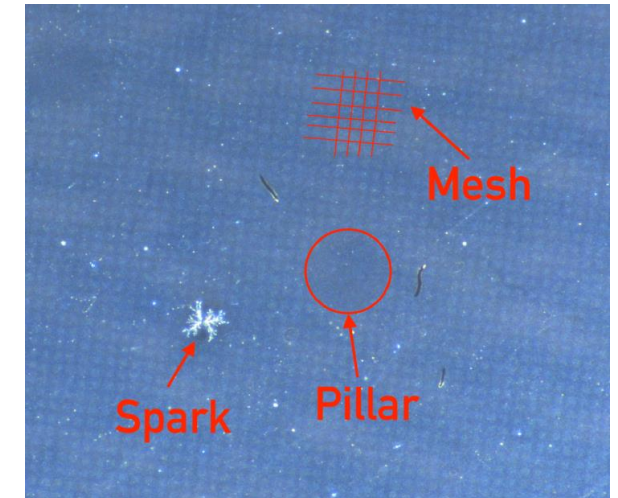
CsI is highly susceptible to degradation from:

- humidity from assembly or possible outgassing of materials, e.g., Kapton
- ion backflow (IBF)
- discharges

To increase robustness, different alternatives to CsI are being investigated:

- **Diamond-Like Carbon (DLC)**
- **Boron Carbide (B_4C)**
- Nanodiamonds
- Carbon nano-structures
- Graphene

CsI photocathode damaged by IBF



CsI photocathode after air exposure



IBF and air exposure observations: L. Sohl, PhD dissertation, <https://universite-paris-saclay.hal.science/tel-03167728/>.

Air exposure observations: M. Lisowska, PhD dissertation, (available soon).

QE ageing studies: M. Lisowska's master thesis, <https://cds.cern.ch/record/2885929>.

DLC as Alternative Photocathodes

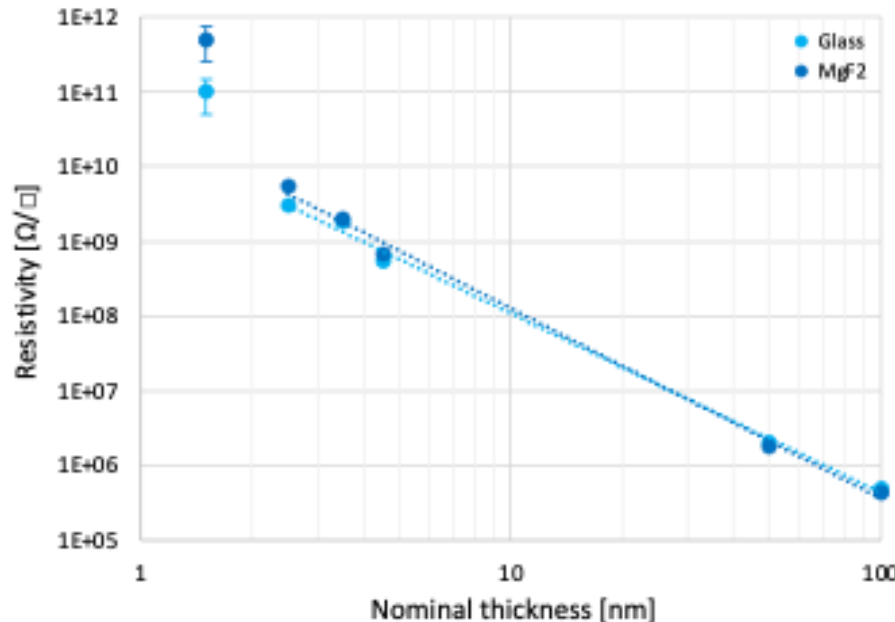
DLC photocathodes, ranging in thickness from 1.5 nm to 3.5 nm, were characterized during the test beam measurements.

The detector with a 1.5 nm DLC layer deposited directly on the radiator exhibited a time resolution of $\sigma = 31.9 \pm 1.3$ ps, while thicker samples showed approximately 4 ps worse resolution.

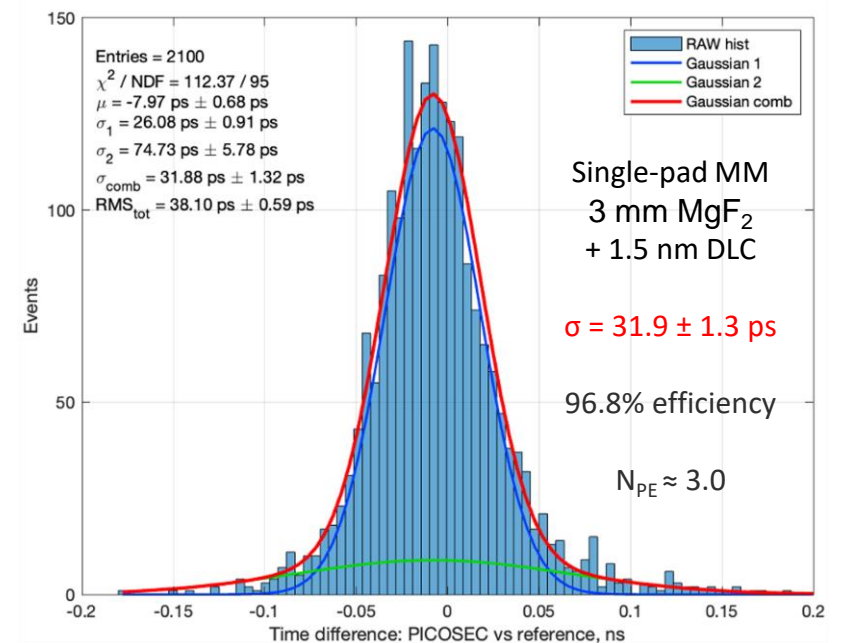
Pulsed DC magnetron vacuum deposition machine



Surface resistivity as a function of layer thickness



Time difference distribution

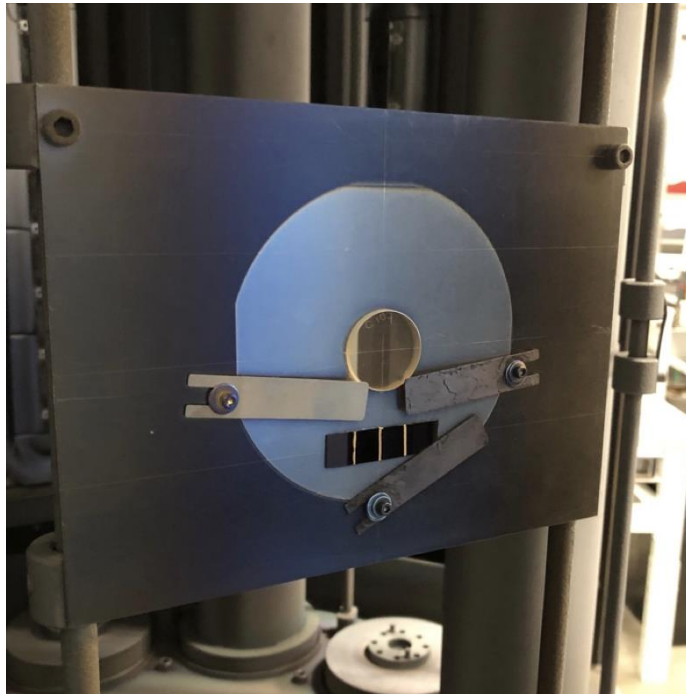


B₄C as Alternative Photocathodes

B₄C photocathodes deposited at CEA-Saclay and ESS have demonstrated promising results.

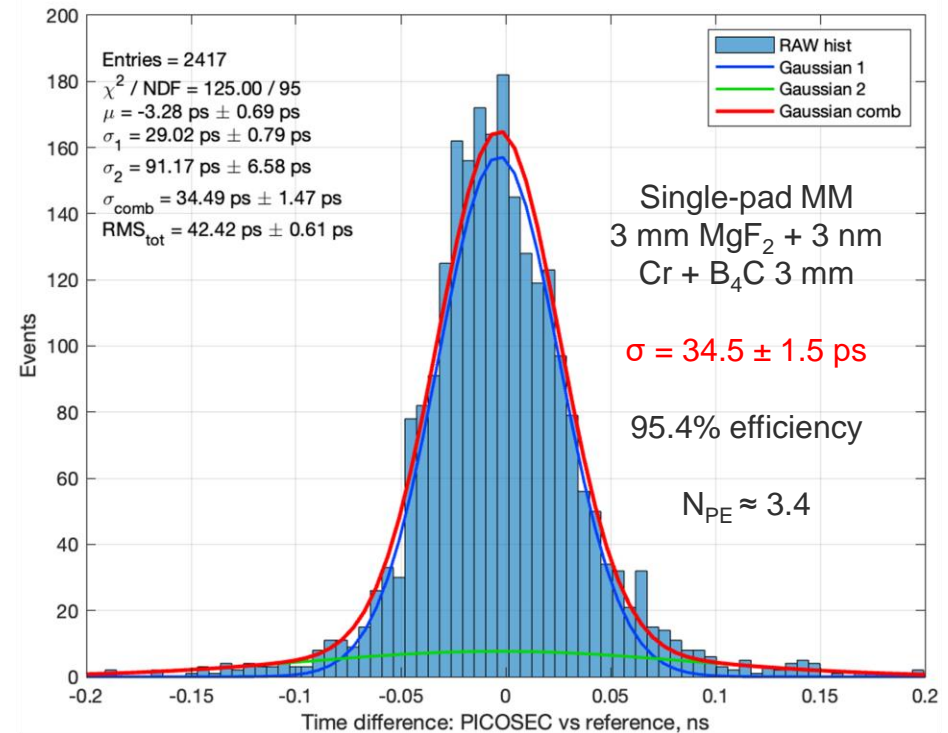
A detector with a 9 nm B₄C layer and 3 nm Cr resulted in a time resolution of $\sigma = 34.5 \pm 1.5$ ps, with thicker samples showing slightly worse resolution by up to ~ 10 ps.

B₄C sample in the sputtering machine



C.-C. Lai, ESS

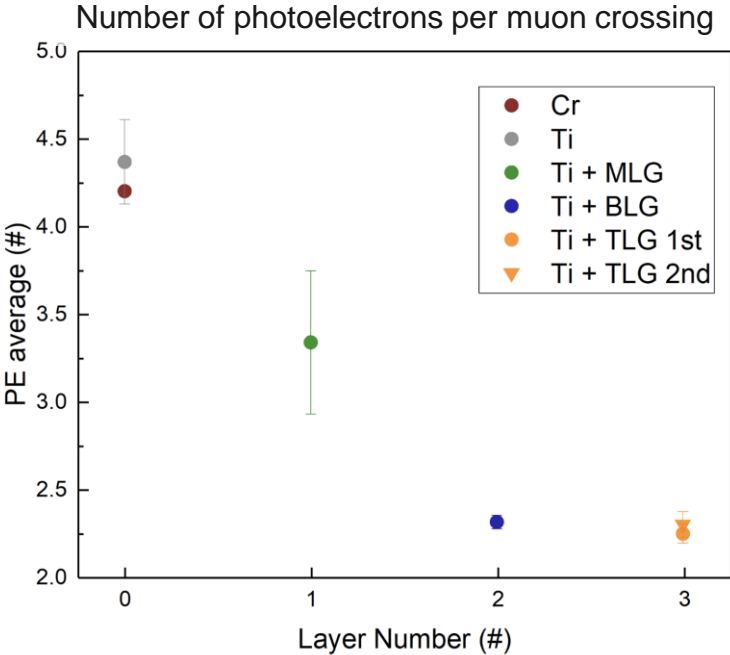
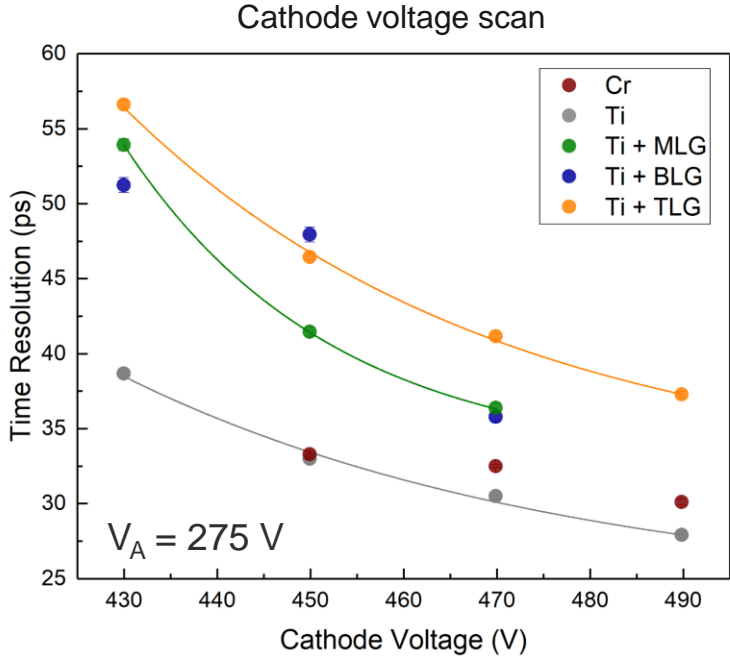
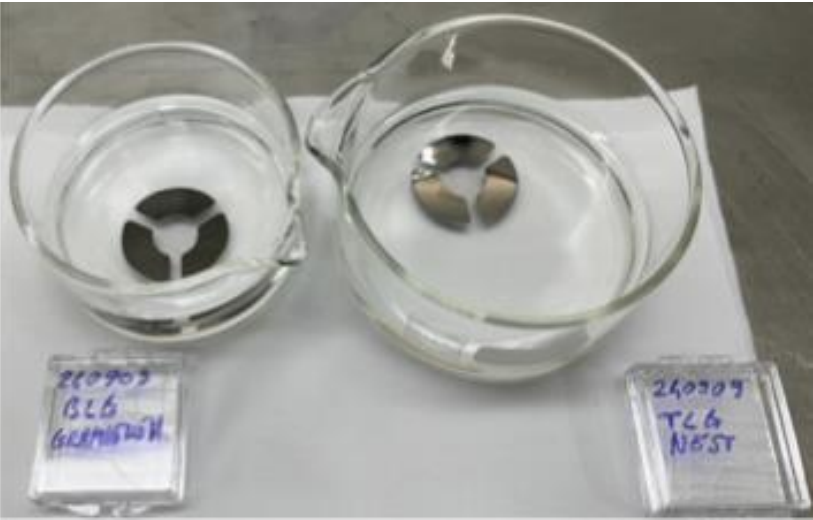
Time difference distribution



Graphene as Protective Layer

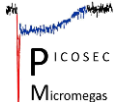
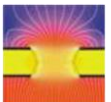
In studies using graphene as a photocathode, a 2.5–3 nm Ti layer produced a surprisingly large number of PEs.

Adding graphene partially screens the photoelectron (PE) emission from the Ti, with the monolayer (ML) screening approximately 30%, and the bilayer (BL) and trilayer (TL) screening about 50% of the PEs.



→ Graphene could be considered as a protective layer.

Towards an applicable detector

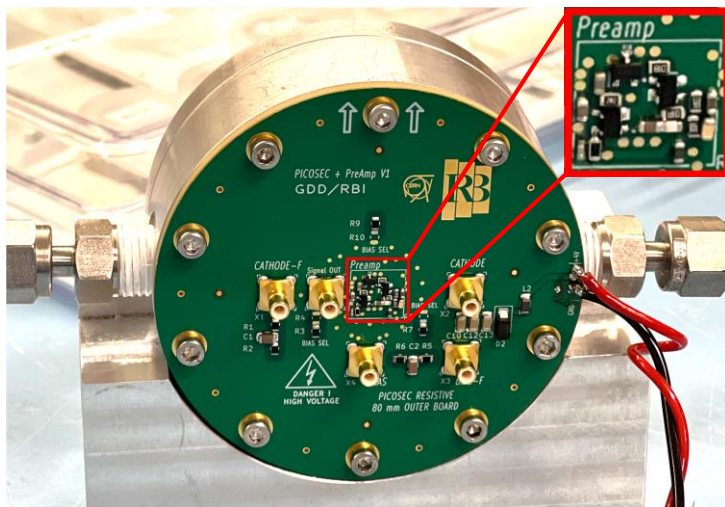


B₄C as an Alternative Photocathodes

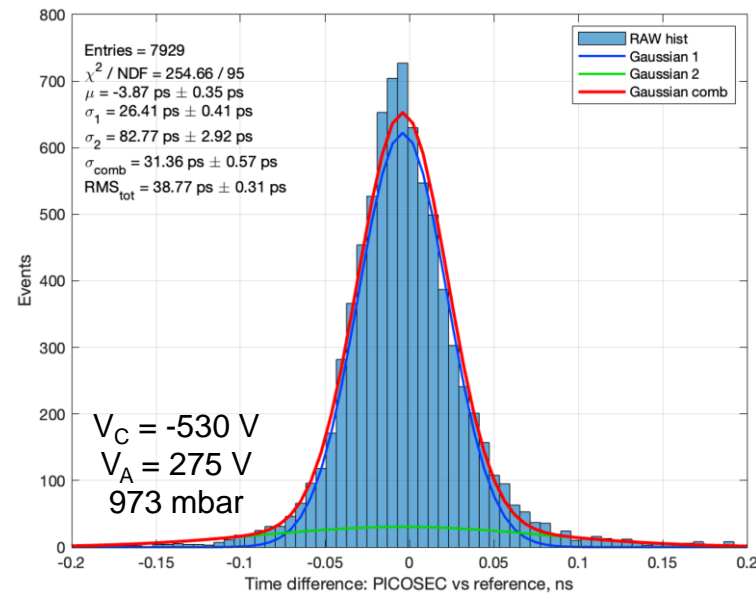
The first measurement combining a single-pad 15 mm ϕ resistive Micromegas + DLC photocathode + embedded amplifier in the outer PCB:

→ showed stable performance and achieved a time resolution of $\sigma = 31.4 \pm 0.6$ ps for fully contained events.

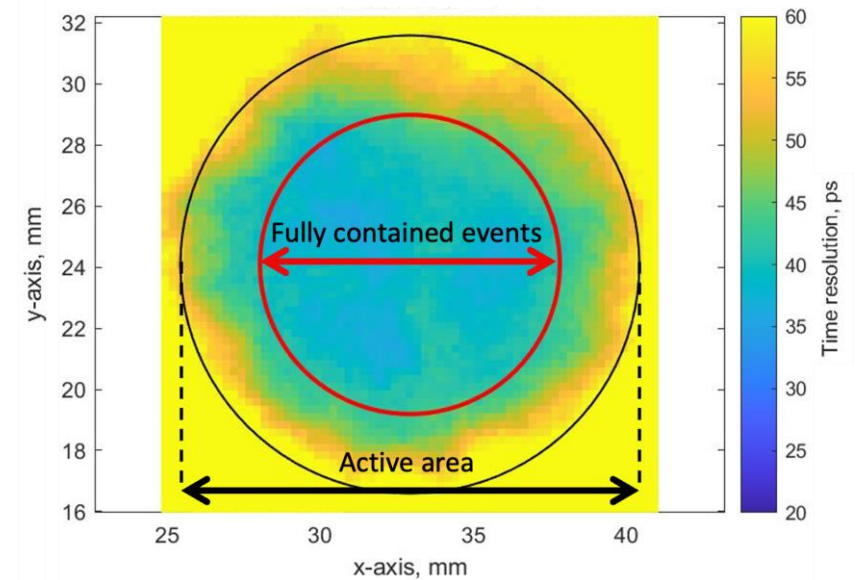
Single-pad detector with the embedded amplifier



Time difference distribution



Time resolution distribution



Summary

To enable the sub-25 ps PICOSEC Micromegas precise-timing detector to perform effectively under the demanding conditions of physics experiments, we are adapting its design to improve robustness.

- **The Resistive Micromegas** with a single-pad and $20 \text{ M}\Omega/\square$ showed equivalent precision to a non-resistive prototype, with time resolution of $\sigma = 12.5 \pm 1.4 \text{ ps}$.
- With **increasing the granularity** of the readout offers the possibility for sub-mm spatial reconstruction, with a pad pitch of 3.5 mm yielding $\sigma = 0.5 \text{ mm}$ with minimal timing degradation in the center of the pad.
- **The vertical charge evacuation design**, while promising ($< 20 \text{ ps}$), needs further investigation to work out non-uniform response.
- Intensive studies for **alternative photocathodes** resulted in achieving a time resolution of $\sigma = 31.9 \pm 1.3 \text{ ps}$ for DLC, $34.5 \pm 1.5 \text{ ps}$ for B_4C , and $36.3 \pm 0.3 \text{ ps}$ for Ti + a monolayer of graphene.

Outlook:

- **Robust photocathodes:** ageing studies of the DLC and B_4C , response to IBF
- **Rate-capability:** double-layer DLC Micromegas for vertical charge evacuation

PICOSEC Micromegas Collaboration

M. Lisowska^{1,2,*}, Y. Angelis³, J. Bortfeldt⁴, F. Brunbauer¹, E. Chatzianagnostou³, K. Dehmelt⁵, G. Fanourakis⁶, K. J. Floethner^{1,7}, M. Gallinaro⁸, F. Garcia⁹, P. Garg⁵, I. Giomataris¹⁰, K. Gnanvo¹¹, T. Gustavsson¹², F.J. Iguaz¹⁰, D. Janssens^{1,13,14}, A. Kallitsopoulou¹⁰, M. Kovacic¹⁵, P. Legou¹⁰, J. Liu¹⁶, M. Lupberger^{7,17}, S. Malace¹¹, I. Maniatis^{1,3}, Y. Meng¹⁶, H. Muller^{1,17}, E. Oliveri¹, G. Orlandini^{1,18}, T. Papaevangelou¹⁰, M. Pomorski¹⁹, L. Ropelewski¹, D. Sampsonidis^{3,20}, L. Scharenberg^{1,17}, T. Schneider¹, L. Sohl¹⁰, M. van Stenis¹, Y. Tsipolitis²¹, S.E. Tzamarias^{3,20}, A. Utrobicic²², R. Veenhof^{1,23}, X. Wang¹⁶, S. White^{1,24}, Z. Zhang¹⁶, and Y. Zhou¹⁶

¹European Organization for Nuclear Research (CERN), CH-1211, Geneva 23, Switzerland

²Université Paris-Saclay, F-91191 Gif-sur-Yvette, France

³Department of Physics, Aristotle University of Thessaloniki, University Campus, GR-54124, Thessaloniki, Greece

⁴Department for Medical Physics, Ludwig Maximilian University of Munich, Am Coulombwall 1, 85748 Garching, Germany

⁵Stony Brook University, Dept. of Physics and Astronomy, Stony Brook, NY 11794-3800, USA

⁶Institute of Nuclear and Particle Physics, NCSR Demokritos, GR-15341 Agia Paraskevi, Attiki, Greece

⁷Helmholtz-Institut für Strahlen- und Kernphysik, University of Bonn, Nußallee 14–16, 53115 Bonn, Germany

⁸Laboratório de Instrumentação e Física Experimental de Partículas, Lisbon, Portugal

⁹Helsinki Institute of Physics, University of Helsinki, FI-00014 Helsinki, Finland

¹⁰IRFU, CEA, Université Paris-Saclay, F-91191 Gif-sur-Yvette, France

¹¹Jefferson Lab, 12000 Jefferson Avenue, Newport News, VA 23606, USA

¹²LIDYL, CEA, CNRS, Université Paris-Saclay, F-91191 Gif-sur-Yvette, France

¹³Inter-University Institute for High Energies (IIHE), Belgium

¹⁴Vrije Universiteit Brussel, Pleinlaan 2, 1050 Brussels, Belgium

¹⁵Faculty of Electrical Engineering and Computing, University of Zagreb, 10000 Zagreb, Croatia

¹⁶State Key Laboratory of Particle Detection and Electronics, University of Science and Technology of China, Hefei 230026, China

¹⁷Physikalisches Institut, University of Bonn, Nußallee 12, 53115 Bonn, Germany

¹⁸Friedrich-Alexander-Universität Erlangen-Nürnberg, Schloßplatz 4, 91054 Erlangen, Germany

¹⁹CEA-LIST, Diamond Sensors Laboratory, CEA Saclay, F-91191 Gif-sur-Yvette, France

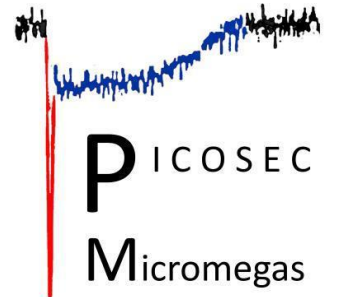
²⁰Center for Interdisciplinary Research and Innovation (CIRI-AUTH), Thessaloniki 57001, Greece

²¹National Technical University of Athens, Athens, Greece

²²Institute Ruder Bosković Institute, Bijenička cesta 54, 10000, Zagreb, Croatia

²³Bursa Uludağ University, Görükle Kampusu, 16059 Niüfer/Bursa, Turkey

²⁴University of Virginia, USA



Thank you for your attention!

